Ultralow-Power Four-Wave Mixing with Rb in a Hollow-Core Photonic Band-Gap Fiber

Pablo Londero,* Vivek Venkataraman, Amar R. Bhagwat, Aaron D. Slepkov, and Alexander L. Gaeta

Department of Applied and Engineering Physics, Cornell University, USA

(Received 2 March 2009; revised manuscript received 25 June 2009; published 23 July 2009)

We demonstrate extremely efficient four-wave mixing with gains greater than 100 at microwatt pump powers and signal-to-idler conversion of 50% in Rb vapor confined to a hollow-core photonic band-gap fiber. We present a theoretical model that demonstrates such efficiency is consistent with the dimensions of the fiber and the optical depths attained. This is, to our knowledge, the largest four-wave mixing gain observed at such low total pump powers and the first demonstrated example of four-wave mixing in an alkali-metal vapor system with a large (~30 MHz) ground state decoherence rate.

DOI: 10.1103/PhysRevLett.103.043602 PACS numbers: 42.50.Gy, 42.50.Nn

Performing nonlinear optics at the single-photon level is critical to the development of quantum networks [1,2] and to fundamental studies of QED effects [3–5]. Alkali-metal vapors are promising for these applications due to the well-defined resonances of these atoms and to the high optical depths that can be attained. A number of interesting quantum and low-light level effects have been observed in such vapors, such as storage and retrieval of quantum states, switching at low photon number [6], quantum nondemolition measurements [3], and quantum noise correlations [7,8].

In order to reach the single-photon limit, it is important to develop alkali-metal vapor systems capable of generating ever-higher effective nonlinearities. A number of features are required in order to create a strong coherent nonlinear response in an alkali-metal vapor at very low photon numbers. One is a strong coupling between the light and the atomic medium. This can be achieved by maximizing $g\sqrt{\mathrm{OD}}/\gamma$, where g is the atom-field coupling constant in units of angular frequency, $\mathrm{OD} = -\ln(T)$ is the optical depth experienced by the spatial light mode, T is the on-resonance transmission, and γ is the excited-state radiative decay rate. Another critical feature is a long spin coherence time, which requires management of various decoherence mechanisms including magnetic fields, inelastic collisions, and radiation trapping.

One approach to enhance light-atom interactions with alkali-metal vapors is to confine light to a waveguide structure where the vapor interacts either with the evanescent tail of the guided mode [9–11] or inside a hollow guiding structure [12,13]. Such a geometry has the benefit of increasing g while permitting interactions over a length much greater than the Rayleigh length of a similar-sized focused spot size. Furthermore, these systems can utilize typical methods for magnetic field control and inherently suppress radiation trapping due to their high aspect ratio [14,15]. Although short spin coherence times can be an issue due to the brief transit time across the beam cross section, it may be possible to ameliorate the problem by trapping the vapor [16,17], by applying a coating to walls of the system cell [18], or by using a buffer gas [19].

We have previously demonstrated the ability to generate large optical depths of Rb vapor inside of a hollow-core photonic band-gap fiber (PBGF) using light-induced atomic desorption (LIAD) [12,20]. PBGFs consist of a Bragg structure surrounding an empty core, typically around 10 μm in diameter. The core supports guided mode propagation for many tens of meters (see Fig. 1). LIAD from the core glass walls causes Rb atoms to desorb from the glass, generating a vapor in the core that can interact with guided fields present in the fiber.

In this Letter, we show that large vapor densities can be produced in this system to generate nonlinear four-wave mixing (FWM) at ultralow pump powers. Efficient frequency conversion and large gain are demonstrated at only microwatts of pump power. FWM experiments, in particular, provide a test bed for measuring the low-light interaction strengths that can be achieved in an alkali-metal system while generating interesting effects such as frequency conversion, gain, optical phase conjugation, and relative intensity squeezing of light modes [21,22].

We investigate FWM in our PBGF-Rb system by employing a double-lambda configuration with ^{85}Rb resonances, as shown in Fig. 2. The basic scheme consists of two ground states coupled to a single excited state by two pump fields. Pump field Ω_1 is on resonance with the $1 \leftrightarrow 3$

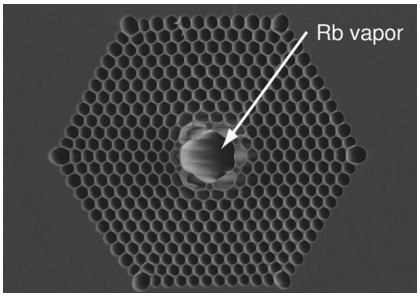

FIG. 1. Transmission electron microscope image of the cross section of the fiber used in these experiments. Light-induced atomic desorption is used to generate rubidium vapor in the core region, which then interacts with light fields coupled into the core.

transition, while pump field Ω_2 is detuned to the blue of the $2 \leftrightarrow 3$ resonance by Δ. The weak signal field E_s is detuned from the $1 \leftrightarrow 2$ Raman transition involving E_s and Ω_2 by the quantity $\delta = \Delta' - \Delta$. This produces an idler field which is detuned from the $1 \leftrightarrow 2$ Raman transition involving E_i and Ω_1 by the quantity $-\delta$.

The system is modeled assuming a thermal density matrix for the ensemble of atomic states, and transit-time broadening effects are added phenomenologically. The resulting Bloch equations are coupled to signal- and idler-field propagation through the susceptibilities of the respective wave equations. The set of equations can then be simplified to yield coupled wave equations for the signal and idler.

Since the atoms in the fiber exhibit inelastic scattering against the fiber walls at a rate of $\gamma_T/2\pi \sim 30$ MHz and have an excited-state decay rate of $\gamma/2\pi = 6$ MHz, the system cannot be optically pumped into a pure state. Thus population in either of the ground hyperfine states $|1\rangle$ and $|2\rangle$ generates FWM incoherently with respect to population in the other hyperfine state. This leads to the following coupled equations between the signal and idler fields that are more complicated than similar systems [23]:

$$\left[\frac{\partial}{\partial t} + c\frac{\partial}{\partial z}\right]E_s = -i\frac{\alpha}{2}[(2A_2 - A_1) + A_1\cos(2\Omega_1 t)]E_i^* - iA_1\frac{\alpha}{2\Omega_1}\left[\gamma_T \sin(2\Omega_1 t) + 2\Omega_1\cos(2\Omega_1 t) + \sin(2\Omega_1 t)\frac{\partial}{\partial t}\right]E_i^* + (A_2 - A_1)\frac{2\eta\gamma_L}{\gamma}\left[\gamma_T + \frac{\partial}{\partial t}\right]E_s, \quad (1a)$$

$$\left[\frac{\partial}{\partial t} + c\frac{\partial}{\partial z}\right]E_i^* = +i\alpha(A_2 - A_1)E_s - \frac{\eta}{2}[(2A_2 - A_1)\gamma_T + A_1\gamma_T\cos(2\Omega_1 t) - 3A_1\Omega_1\sin(2\Omega_1 t)]E_i^* - \frac{\eta}{2}[(2A_2 - A_1) + A_1\cos(2\Omega_1 t)]\frac{\partial}{\partial t}E_i^*, \quad (1b)$$

where γ_T is the inverse of the atomic transit time, $\Omega_{1(2)}$ is the Rabi frequency of the corresponding field in Fig. 2, $\eta = g^2N/|\Omega_1|^2$, $g = d_{32}\sqrt{\omega_{32}/2\hbar\epsilon_0 V}$ is the atom-field coupling constant, d_{32} is the dipole moment of the $3 \leftrightarrow 2$ transition, ω_{32} is the angular frequency of the $3 \leftrightarrow 2$ transition, V is the quantization volume, N is the number of atoms, $\alpha = \eta\Omega_1\Omega_2/\Delta$, $\gamma_L = \gamma|\Omega_2|^2/2\Delta^2$, and $A_1 = 1/2 - \gamma/8\gamma_T$ and $A_2 = 1/2 + \gamma/8\gamma_T$ are the average steady-state populations of states $|1\rangle$ and $|2\rangle$, respectively.

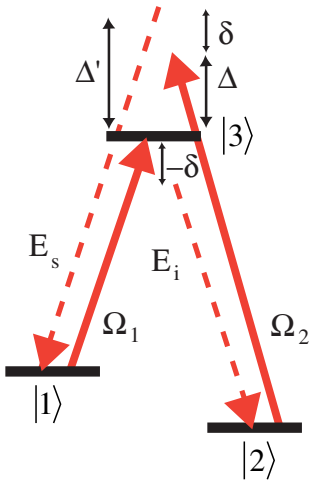

FIG. 2 (color online). Energy-level diagram of the FWM scheme. Pump fields of Rabi frequency Ω_1 and Ω_2 mix with the signal field E_s and the generated corresponding idler field E_i. Pump Ω_1 is on resonance, while Ω_2 is blue-detuned from the excited state by Δ. The signal field is detuned from the excited state by Δ' and thus from the two-photon Raman resonance by $\delta = \Delta' - \Delta$. This generates an idler field E_i which is detuned from its Raman resonance by $-\delta$.

Taking the limiting case of cold atoms ($A_1 = 0$, $A_2 = 1$, $\gamma_T = 0$), we note that one recovers expressions for FWM in a pure state [23]. In the full thermal case, the presence of population in both states leads to a variety of effects. The signal and idler are cross coupled by a number of terms proportional to α which generate FWM. Raman gain and loss are represented by the terms proportional to η. The presence of sinusoidal terms is due to population in state $|1\rangle$, which oscillates at the Rabi frequency of the resonant pump field.

The FWM interaction in our PBGF-Rb system is realized experimentally using the ^{85}Rb $5\,^2S_{1/2}$ to $5\,^2P_{1/2}$ (D1) transitions. The $F = 2$ and $F = 3$ states associated with the $5\,^2S_{1/2}$ are separated by 3 GHz and serve as the ground states of the system. The excited-state interaction takes place with both the $F' = 2$ and $F' = 3$ states of the $5\,^2P_{1/2}$, which are separated by 360 MHz and are thus within each others' Doppler-broadened profile. Pump Ω_2 is detuned 1 GHz above the $|2\rangle \leftrightarrow |3\rangle$ transition, and Ω_1 is tuned in between the $F' = 2$ and $F' = 3$ transitions.

The setup for generating and measuring FWM is shown in Fig. 3. We use a 30-cm PBGF (Crystal Fibre AIR-6-800, 6 μm core, ~3 μm FWHM fundamental field mode) that links two vacuum cells with a Rb source attached to one of the cells, as described in previous experiments by our group [12]. The pump beams are combined with a probe beam that acts as the signal field E_s, using a polarization beam splitter (PBS) cube at the input of the PBGF. This ensures that the polarizations of the pump and probe fields are orthogonal (see Fig. 3). All three beams are on con-

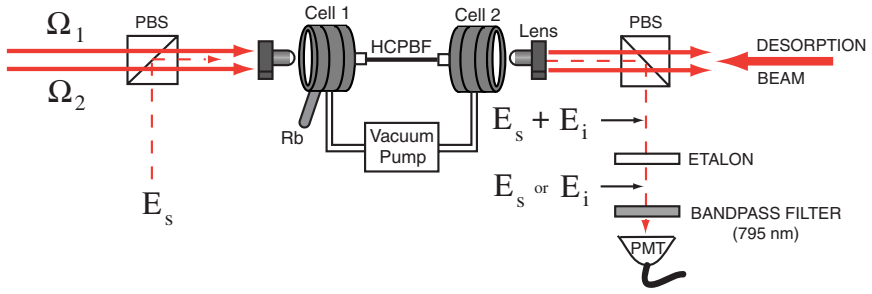

FIG. 3 (color online). Experimental setup for the FWM experiments. Pump fields Ω_1 and Ω_2 are combined with a cross-polarized signal field on a PBS propagate collinearly through the PBGF. The fiber is sealed to two vacuum cells, the leftmost of which contains Rb vapor which enters the core of the fiber and attaches to the fiber walls. The vapor density is controlled by a counterpropagating desorption beam of a chosen duration and power. The signal and idler fields are separated from the pump fields by a PBS and from each other by an etalon.

tinuously. We desorb with 3 mW of power at 808 nm (detuned far from any Rb resonances) coupled into the PBGF counterpropagating to the pump and probe waves. The desorbing beam is pulsed with an acousto-optic modulator for the duration necessary to generate the desired OD in the fiber, typically between 1 and 2.5 seconds.

The frequency of the probe field E_s is scanned over 1.5 GHz at a rate of 10 Hz about the two-photon Raman resonance at $\delta = 0$, and the signal (E_s) and idler (E_i) powers are measured. The signal and idler fields are separated from the pump waves using a PBS cube at the output of the fiber. A temperature-controlled etalon (with a free spectral range of 40 GHz and a finesse of 100) is then used to selectively transmit either of the fields onto a photomultiplier tube (PMT) (Hamamatsu H7422-50). The output of the PMT was integrated into 100 μs time bins. A 795-nm bandpass filter in front of the PMT serves to remove any backscatter from the desorption beam. We note that the continuous pump and signal field, 1–2.5 s desorption pulse, the signal field scanning rate given above, and the 100 μs integration time of the PMT output imply that these measurements are performed in the steady-state limit of Eqs. (1a) and (1b).

Our results are shown in Fig. 4. A high OD is generated in the fiber by a 3-mW, 1-s-long desorption pulse. Figure 4(a) shows the probe transmission as it is scanned across the D1 transition. Fitting the Rb resonances to the OD profile, taking into account transit-time broadening, and allowing temperature to vary, we estimate an OD = 20 on resonance. In the presence of the pump waves, the signal field acquires gain when it is two-photon resonant with Ω_2 [Fig. 4(c)]. We observe a signal field gain factor of 6 with 15 μW of total pump power at a power ratio of $\|\Omega_2\|^2:\|\Omega_1\|^2 = 2{:}1$. When the etalon is set to transmit the idler field, we observe the power of the generated idler beam [see Fig. 4(b)] to be 50% that of the input probe. The idler field is not observed if any of the input fields are blocked, which corroborates that the FWM process is present inside the fiber.

We compare these data to a numerical integration of Eqs. (1a) and (1b), which represents an approximate description of the experiment and which allows us to draw some general conclusions. Doppler broadening is not included, which affects the detuning of Ω_2 and introduces a detuning for Ω_1. We assume the pump beams are not absorbed by the medium since they are approximately 10^4 times the saturation intensity of rubidium vapor. Inserting our experimental parameters and allowing only the atom number in the fiber to vary, we find the model predicts a gain of 6 for $N = 2.3 \times 10^5$ atoms. This value is

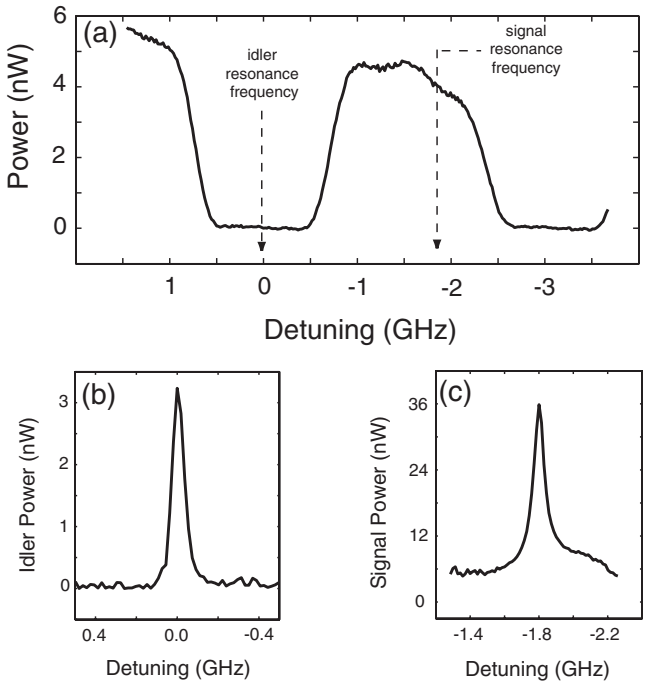

FIG. 4. (a) Probe transmission through the fiber as its frequency is scanned across the D1 line after generating a Rb vapor by desorption. (b) Idler power versus frequency as detected while scanning the probe detuning. (c) Gain experienced by the signal field as a function of detuning.

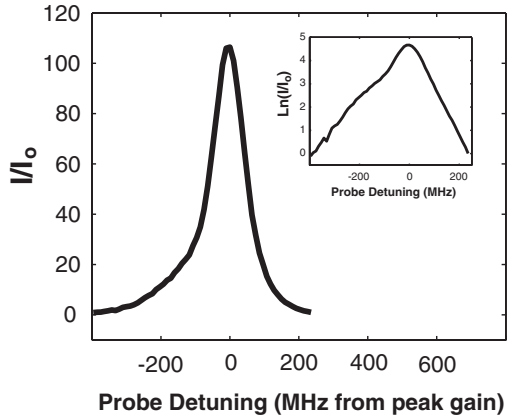

FIG. 5. Probe gain for Rb vapor generated from a 2.5-s desorption pulse. A gain of more than 100 is observed. Inset: At lower gains, the bandwidth can exceed 300 MHz.

reasonable when compared to the number of atoms required to fit to the absorption profile of Fig. 4(a), which we found to be 5.2×10^5 and suggests that the observed gain is consistent with the magnitude one expects from FWM in the system.

At larger ODs and slightly larger pump powers, we observe dramatically higher gain at the probe transition. As shown in Fig. 5, a 2.5-s desorption beam and 36 μW of total pump power yield a peak gain of 105. The logarithmic plot of the gain curve shows that this imaginary component of the susceptibility is present over the 3-dB bandwidth of 300 MHz, which is capable of supporting 500-ps pulses. These gain efficiencies and bandwidth values are many orders of magnitude greater than similar experiments in bulk vapor cells. Hemmer *et al.* used a similar scheme in sodium vapor to observe a gain of 55 and response times of $\sim$1 μs using 10 mW of pump power [21]. Boyer *et al.* observed a gain of 30 and bandwidth of $\sim$10 MHz in rubidium vapor using 280 mW of pump power [24], though it should be noted that their double-lambda scheme used a degenerate pump that was off-resonance from all transitions.

Numerical integration of the propagation equations yields an equivalent gain at 4.5×10^5 atoms, which is only twice that required for a gain of 6. This may be due not only to the exponential increase in gain as a function of N but also to the transition into the high-gain regime, where the loss terms are weak compared to the cross-coupling strength. The observed effective nonlinearity is limited primarily by the number of atoms in the core and transit-time broadening, which is evident from Eqs. (1a) and (1b). The cross-coupling coefficient α is proportional to the number of atoms, and the magnitude of the DC cross-coupling terms increases as γ_T decreases.

We have also observed weak gain (data not shown) using the scheme of McCormick *et al.* [22] where all pump, signal, and idler fields are off-resonance and away from any absorption. This is particularly intriguing since it can, in principle, produce a high degree of nonclassical correlation even at low gain and so may be usable for generation of correlated photon pairs. This regime will be the object of further study in the future.

There are a number of improvements that could further increase the nonlinearities we observe. Recent experiments on a redesigned PBGF-Rb chamber [20] show that it may be possible to produce atomic densities more than an order of magnitude larger than those presented in this Letter. One would expect the imaginary component of the susceptibility to increase accordingly. Another approach is to produce a purer state among the ground hyperfine levels by increasing the transit time, such as by injecting buffer gas into the PBGF.

In summary, our measurements show that this system can achieve extremely efficient nonlinearities, with FWM gains $>$100 at only 36 μW of total pump power. As such, this fiber-based system shows promise for studying other novel nonlinear optics effects such as classical and quantum noise correlations and dispersive effects from electromagnetically induced transparency and gain resonances, at ultralow-light levels and with exceptionally high bandwidths for an alkali-metal vapor system.

*pl336@cornell.edu

[1] J. O'Brien *et al.*, Science **318**, 1567 (2007).
[2] D. Petrosyan *et al.*, J. Opt. B **7**, S141 (2005).
[3] H. Schmidt and A. Imamoglu, Opt. Lett. **21**, 1936 (1996).
[4] I. Schuster *et al.*, Nature Phys. **4**, 382 (2008).
[5] A. S. Parkins *et al.*, Science **319**, 1062 (2008).
[6] D. Braje *et al.*, Phys. Rev. A **68**, 041801(R) (2003).
[7] M. D. Lukin *et al.*, Phys. Rev. Lett. **82**, 1847 (1999).
[8] A. S. Zibrov *et al.*, Phys. Rev. Lett. **83**, 4049 (1999).
[9] F. L. Kien *et al.*, Phys. Rev. A **72**, 032509 (2005).
[10] T. Aoki *et al.*, Nature (London) **443**, 671 (2006).
[11] S. M. Spillane *et al.*, Phys. Rev. Lett. **100**, 233602 (2008).
[12] S. Ghosh *et al.*, Phys. Rev. Lett. **97**, 023603 (2006).
[13] W. Yang *et al.*, Nat. Photon. **1**, 331 (2007).
[14] R. Stites *et al.*, Opt. Lett. **29**, 2713 (2004).
[15] A. B. Matsko *et al.*, Phys. Rev. Lett. **87**, 133601 (2001).
[16] S. Chu *et al.*, Phys. Rev. Lett. **57**, 314 (1986).
[17] T. Takekoshi and R. J. Knize, Phys. Rev. Lett. **98**, 210404 (2007).
[18] J. C. Camparo *et al.*, J. Chem. Phys. **86**, 1533 (1987).
[19] W. Happer *et al.*, Rev. Mod. Phys. **44**, 169 (1972).
[20] A. D. Slepkov *et al.*, Opt. Express **16**, 18 976 (2008).
[21] P. R. Hemmer *et al.*, Opt. Lett. **20**, 982 (1995).
[22] C. F. McCormick *et al.*, Opt. Lett. **32**, 178 (2007).
[23] A. Axel, *Nonclassical States of Light and Atomic Ensembles* (Harvard University, Cambridge, MA, 2005).
[24] V. Boyer *et al.*, Phys. Rev. Lett. **99**, 143601 (2007).